Water Practice & Technology

IWA PUBLISHING

Water Practice & Technology Vol 17 No 1, 297 doi: 10.2166/wpt.2021.105

Development of nano-activated carbon and apply it for dyes removal from water

Layla A. Al Jebur[a,*] and Liqaa Hussein Alwan[b]

[a] Department of Chemistry, College of Science, Tikrit University, Tikrit, Iraq
[b] Department of Chemistry, College of Education, University of Samarra, Samarra, Iraq
*Corresponding author. E-mails: layla.a.jaber@tu.edu.iq; abudlayla@gmail.com

ABSTRACT

The present study investigates the production of nano-activated carbon from banana peels mixed with nylon 6.6 and polyethene. The carbonization process was carried out by mixing accurate percentages of the banana peels with different ratios of nylon 66 and a suitable amount of potassium hydroxide. The fusion carbonization, without solvents, was used in this paper to decompose the nylon mixture, releasing amino and carboxylate roots that can easily react with the carbon chains. The prepared nano-activated carbon was characterized using different technologies, including SEM, AFM, FT-IR, and EDX technologies. The results showed the produced carbon has spherical particles with a pore size of 1.21 nm and a surface area of 1,071.7 m^2/gm. Additionally, it was noticed, from the FT-IR spectrum, the prepared carbon does not contain any active groups, which means it is an inert material. X-ray analysis showed the new carbon is made from carbon (78.57%) and oxygen (21.43%). After optimizing the wavelength, the prepared carbon was used to adsorb methylene blue and Eirochrom black T dyes from solutions. The results showed the best equilibrium time, dose of carbon and concentration of dyes was 40–50 minutes, 0.04 g and 20 ppm, respectively.

Key words: dyes removal, nano-activated carbon, water

HIGHLIGHTS

- Nano-activated carbon was made from banana peels, nylon 6.6 and polyethene.
- The new carbon has a surface area of 1071.7 m^2/gm.
- Nano-activated carbon removed dye after 40–50 minutes.

GRAPHICAL ABSTRACT

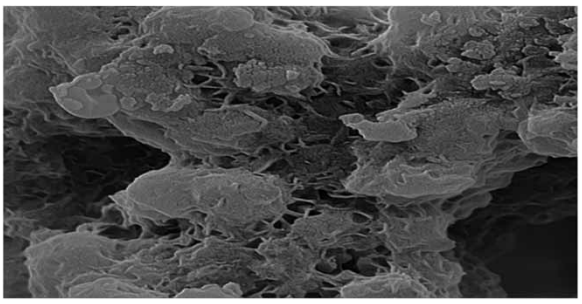

1. INTRODUCTION

The global population is increasing at a fast pace, especially in the last centuries due to the enhancement in medication and the economy. This increase in the population was accompanied by a similar increase in industry and agriculture (Abdulhadi *et al.* 2019; Aqeel *et al.* 2020) and the urbanization process (use of the land) (Al-Jumeily *et al.* 2019; Farhan *et al.* 2019, 2021). Thus, as a result of this increase, the production of wastewaters either from agriculture (Hashim *et al.* 2018; Al-Saati *et al.* 2021) or industry (Zubaidi *et al.* 2019; Emamjomeh *et al.* 2020b). In fact, the effects of this increase are not limited to water pollution; these activities (agricultural and industrial ones) have seriously contributed to air pollution (Grmasha *et al.* 2020; Al-Sareji *et al.* 2021), which in turn resulted in global warming and droughts (Salah *et al.* 2020b, 2020c). For example, the recent investigations

are indicating serious changes in rain patterns (Zubaidi *et al.* 2020a, 2020b) and also a shortage in water (Salah *et al.* 2020a; Zubaidi Salah *et al.* 2020). Therefore, the need for water/wastewater treatment technologies increased more than ever before (Mohammed *et al.* 2020; Omran *et al.* 2021). For example, electrocoagulation (Hashim *et al.* 2019a), filtration (Abdulla *et al.* 2020), coagulation using chemical coagulants (Alenazi *et al.* 2020), or natural coagulants (Al-Saati *et al.* 2019), assisted filtration (Alhendal *et al.* 2020), such as the combination of electrocoagulation and filtration (Emamjomeh *et al.* 2020a). Although some methods, such as electrocoagulation (Hashim *et al.* 2020c) and filtration (Hashim *et al.* 2021b), the adsorption method has brought more attention due to its affordability and effectiveness (Abdulraheem *et al.* 2020; Alenezi *et al.* 2020).

Several natural and waste materials are currently used to develop activated carbon, such as wood, bones, brown and dark coal, peels of coconuts, wastes of refinery products, sugar, and sludges of water treatment plants. Additionally, some synthetic materials, such as polymers, are currently used as adsorption media. Generally, high carbon content materials are favourable in the production of activated carbon as these materials do not require expensive processes to produce the activated carbon (Al-Hashimi *et al.* 2021). While low carbon content materials require a carbonization process at elevated temperatures ranging between 400 and 500 °C to remove unwanted materials (will be volatilized), then the materials pass through the activation process to increase the adsorption capacity. For example, Stoeckli (1990) developed activated carbon from charcoal by reacting it with sodium and potassium hydroxides and then activated the carbon at a temperature of 950–1,000 °C in the presence of argon gas. The developed carbon showed excellent adsorption properties and high surface area. Zhongfu (1991) investigated the preparation of activated carbon from the by-products of the furfural industry; the latter was dried first at a temperature between 80 and 200 °C for 2–8 hours. Then, the dried materials were carbonized at a temperature of 300–500 °C for 2–5 hours, followed by an activation process using water vapour at 800–1,000 °C. Zhong *et al.* (2012) used the peels of peanuts to prepare activated carbon; the peels were cleaned and heated using a microwave oven (500 W) for 8.9 minutes in the presence of phosphoric acid, a similar trial was made by Foo & Hameed (2009) to develop activated carbon from agricultural wastes. The authors used peels of pineapples to prepare the activated carbon; the peels were heated in a microwave oven (600 W) for 6 minutes in the presence of potassium hydroxide and potassium carbonate. The preparation of activated carbon was not limited to agricultural wastes, but petroleum wastes were also used in this field. For example, asphalt plant wastes with polymers to develop activated carbon. The mixture was subjected to thermal and chemical activations; the thermal activation included the addition of potassium hydroxide, while the heating process was carried out using conventional and microwave sources.

The activated carbon is divided into two types, according to the shape of its particles, which are powder activated carbon and spherical activated carbon; the spherical type is usually used in adsorption of gases, while the powdered one is used in liquids (Abatan *et al.* 2019). According to the activity, the removal of pollutants on the activated carbon is usually divided into four types, namely adsorption, surficial reactions, ion exchange, and mechanical filtration (Taha *et al.* 2016).

Generally, activated carbon is manufactured from materials with high carbon content, such as wood, brown and dark charcoals, petroleum charcoal, cellulosic materials, and some polymers (Lim *et al.* 2010). Wood is the most used material in activated carbon production because of its availability and high content of cellulose, lignin, and hemicellulose. Therefore, many studies have employed wood in different industries, such as petrochemical products, fuel and activated carbon (Ekpete *et al.* 2017). For example, Yamaguchi *et al.* (2019) produced activated carbon by adding some alkaline materials to the lignin, then treated the mixture thermally at a temperature of 600 °C. The produced activated carbon had excellent adsorption properties. Activated carbon was also produced from wood by adding sodium acetate to softwood and treated them thermally at a temperature of 450 °C; the products of the thermal treatment were activated using water vapour at 1,000 °C (Rahimian & Zarinabadi 2020).

The problem with activated carbon production is the appearance of different-sized pores in the structure of the activated carbon during the manufacturing process, which affects the adsorption process. Generally, the activated carbon has a large surface area ranging between 300 to 2,000 m^2/gm and could reach 5,000 m^2/gm in some cases (Ozdemir *et al.* 2014; Efeovbokhan *et al.* 2019).

Dyes are considered one of the main sources of water pollution due to their wide use in different industries, such as textile, printing, petroleum, backing and food industries. Additionally, the amounts of dyes used in the mentioned industries are relatively high compared to other materials, where the wasted dyes represent 10 to 15% of the total industrial wastes. The problem of dye contamination of water is the variety of dyes' chemical

compositions. Indeed, this problem is one of the most significant problems at the current time due to the importance of water for humans and also for industry. Therefore, water pollution with dyes needs special attention and reliable treatment.

Many treatment methods have been used to remove dyes from water, including electrocoagulation (Hashim *et al.* 2019b), filtration (Abdulraheem *et al.* 2020), coagulation using chemical coagulants (Omran *et al.* 2019), or natural coagulants, and assisted filtration, such as the combination of electrocoagulation and filtration (Alyafei *et al.* 2020). Although many researchers claimed electrocoagulation as very efficient (Hashim *et al.* 2020b), affordable and able to eliminate many pollutants in a short time (Hashim *et al.* 2020a; Zanki *et al.* 2020), there are many serious facts reported about the performance of electrocoagulation, such as the effects of organic matter on the removal of pollutants (Abdulhadi *et al.* 2021; Hashim *et al.* 2021a). That forces the researchers to combine the electrocoagulation method with other technologies, such as ultrasonic (Al-Marri *et al.* 2020; Alnaimi *et al.* 2020). Therefore, the adsorption method has brought more attention.

The adsorption method is the most widely used in this field of treatment due to its high efficiency and affordable cost in comparison with other methods (Alyafei *et al.* 2020). The application of the adsorption method in removing dyes from water dates back to the 70 s of the last century when activated carbon and charcoal were used to remove acidic and alkaline dyes from solutions.

For example, El-Sayed *et al.* (2014) used the activated carbon from different sources to adsorb dyes from solutions. The used activated carbon was derived from charcoal, silica, alumina and kaolin. The results showed the excellent efficiency of the activated carbon to remove dyes, and it was noticed that the best equilibrium time ranged between 90 and 100 minutes, and the adsorption was exothermic and with low randomness. Abdullah *et al.* (2020) produced activated carbon from lemon leaves and used it for the removal of Eriochrome dye from water and found the equilibrium time was 30 to 35 minutes when the dose was 0.05 grams. The results showed the adsorption increases with the increase of the contact time, and the adsorption was exothermic. Additionally, nano adsorption is widely used in other applications, such as human health, sterilization and purification of water.

In this context, the present study aims at the production of activated carbon from banana peels by mixing them with nylon 6.6 and polyethene. The main physical properties of the produced activated carbon will be examined, in this study, using SEM, AFM, FT-IR, and EDX technologies. Then the activated carbon will be used to adsorb methylene blue and Eirochrom black T (EBT) dyes from solutions.

2. EXPERIMENTAL WORK

2.1. Materials and chemicals

The used materials and chemicals in this study were banana peels, sodium hydroxide (0.1 N), hydrochloric acid (0.1 N), nylon polyethene and methylene blue dye, EBT dye, [1-hydroxy-2 naphthol azo]-6-nitro, Naphthol-4-sulphonic acid sodium salt, and $HOC_{10}H_6N = NC_{10}H_4$ (OH) (NO_2) SO_3Na). These chemicals were supplied from Aldrich and Fluka companies.

Several devices were used in this study to achieve the planned goals. A UV spectrophotometer (Shimadzu, 1650PC) and FT-IR spectrophotometer (Shimadzu, 1S-IR Affinity) were used to measure the wavelengths. Additionally, a shaking water bath (YCW012S), drying and incineration ovens, Atomic Force Microscope (AFM), Scanning Electron Microscope (SEM), Energy-dispersive X-ray spectroscopy and Fourier-transform infrared spectroscopy (FT-IR).

2.2. Preparation of activated carbon

Initially, the peels of banana were cleaned and dried in their natural states; then they were ground into a powder. The powder was firstly placed in a clean steel container, then NaOH solution and nylon 66 were added to the container at different ratios 0.1:2:2, 0.2:2:2, 0.3:2:2, and 0.4:2:2 (NaOH: Nylon 66: Peels of banana). The mixtures were heated at 300 °C for 30 minutes with continuous stirring. This process is the initial carbonization, which was followed by heating the mixture at 550 $\pm$ 25 °C for 90 minutes. Then, the mixture was left to cool down. The produced activated carbon was washed several times with deionized water to remove the alkaline materials, then washed with hydrochloric solutions to remove unwanted ions. Finally, the sample was washed with deionized water to make sure that all unwanted materials were removed. The clean activated carbon was dried at a temperature of 110 °C before grinding it. The activated carbon powder was saved in airtight containers to be used later, see Figure 1.

Figure 1 | The prepared activated carbon samples.

2.3. Measurements of the activity of the activated carbon

2.3.1. Surface area

2.3.1.1. Measurement of the surface area using iodine adsorption method. The surface area of the prepared activated carbon was measured using the iodine adsorption from the solution. This method was used in this study because it is widely used in the literature. This method measures the surface area depending on the number of the adsorbed ions of iodine on 1 gram of activated carbon. In this study, 0.2 grams of the activated carbon was mixed with 2 mL of HCl (5%) and heated for 30 minutes, cooled down to room temperature, and mixed with 100 mL (0.1 N) of iodine solution mixed for 30 minutes using a shaker. Then, 50 mL of the mixed solution was filtered and pipetted out with anhydrous sodium thiosulfate (0.1 N) in the presence of a Starch indicator; the used volume of anhydrous sodium thiosulfate from the pipette.

Iodine number is calculated by calculating the adsorbed weight of iodine by the activated carbon as follows:

$$X = A - [2.2B \times V] \tag{1}$$

$$A = N1 \times 12{,}693 \tag{2}$$

$$B = N2 \times 126.93 \tag{3}$$

where X is the adsorbed weight of iodine (in mg), V is the volume of anhydrous sodium thiosulfate (0.3), $N1$ is the molarity of the iodine solution (0.1), and $N2$ the molarity of the anhydrous sodium thiosulfate (0.1).

Then, the iodine number (1N) is calculated as follows:

$$1N = \frac{1.6\,X}{M.D} \tag{4}$$

where M and D are the weight of the activated carbon and the correction coefficient (which has a value close to 1), respectively.

2.3.1.2. Measurement of the surface area using methylene blue adsorption method. This method is also widely used in the literature; it was performed by mixing 0.1 mg of the activated carbon in a container and then 20 ppm of dye solution and mixed using a shaker for 25 hrs at room temperature. When no change in the colour is noticed, the solution is separated by leaving it to settle down. The separated solution is placed in the adsorption cell and measure the adsorption at a wavelength of 665 nm. Then, the adsorbed amount of dye on the activated carbon using the pre-prepared standard calibration curve. The latter was prepared by measuring the adsorption for different concentrations of methylene blue dye (5, 10, 15, 20 and 25 ppm) at the same wavelength (665 nm).

2.3.2. Measurement of the moisture content

The moisture content was measured by exposing the activated carbon to the atmosphere of the laboratory for 24 hrs and then drying it at 110 °C for 2 hrs. Then, the sample was left to cool down and the difference between the wet and dry weights measured.

2.3.3. Percentage of ash

A measured weight of the activated carbon (1 gram) was placed in a ceramic container and heated at 1,000 °C for 60 minutes and then cooled down to the temperature of the laboratory. The weight of the residual weight was calculated, which represented the weight of the ash.

2.3.4. Measurement of carbon density

A measured weight of the activated carbon was placed in a bottle, 5 mL capacity, and pressed gently to reduce and remove spaces between activated charcoal particles. The surface of the activated carbon in the bottle was levelled according to the mark on the side of the bottle, then the weight of carbon was measured, and the density was calculated as follows:

$$\text{Density}\left(\frac{g}{\text{cm}^3}\right) = \frac{\text{Mass}}{\text{Volume}} \tag{5}$$

2.3.5. Adsorption

The adsorption of EBT dye from the water was done using the developed activated carbon, taking into account the effects of several factors, such as the equilibrium time and dose of the adsorbent. Initially, the maximum wavelength was measured using the dye solution, and the results were used to develop a standard calibration curve. The results showed the maximum wavelength was 528 nm for the tested solution (containing 5–65 ppm). The relationship between the wavelength and concentration of dye is a linear relationship according to the Lambert-Beer law.

3. RESULTS AND DISCUSSION

3.1. Characterization of the nano-activated carbon

The characterization of the nano-activated carbon was done using different technologies, such as:

3.1.1. Fourier transformed infrared (FT-IR)

The FT-IR technology was used in this study to characterize the surface of the developed carbon. This test helps to identify the active groups on the surface of the carbon. The results of characterization are shown in Figure 2.

The FT-IR spectrum results show there are no active groups that may affect the adsorption process; thus, it can be concluded that the nano-activated carbon is chemically inert. This fact makes the developed activated carbon favourable for the adsorption process.

3.1.2. Atomic force microscope (AFM)

The results of the AFM analysis of the surface of the nano-activated carbon are shown in Figure 3, which shows a 3D picture of the activated carbon. It can be seen from this figure many sharp protrusions with heights that could reach up to 99.83 nm, which gives a high surface area for the carbon.

The SEM technology, with a magnifying ratio of 500, was used to study the structure of the new activated carbon; the results of the SEM are shown in Figure 4.

3.1.3. Scanning electron microscope (SEM)

It was noticed from the SEM images that the surface of the prepared activated carbon was rich in voids, cracks, cuts and different sizes of particles were noticed on the surface of the activated carbon, making the structure of this material porous. These voids, cuts and cracks are attributed to the effect of the arsenic chloride that acts to remove water from the fresh material (of cellulose, lignin, and hemicellulose) during the carbonization process.

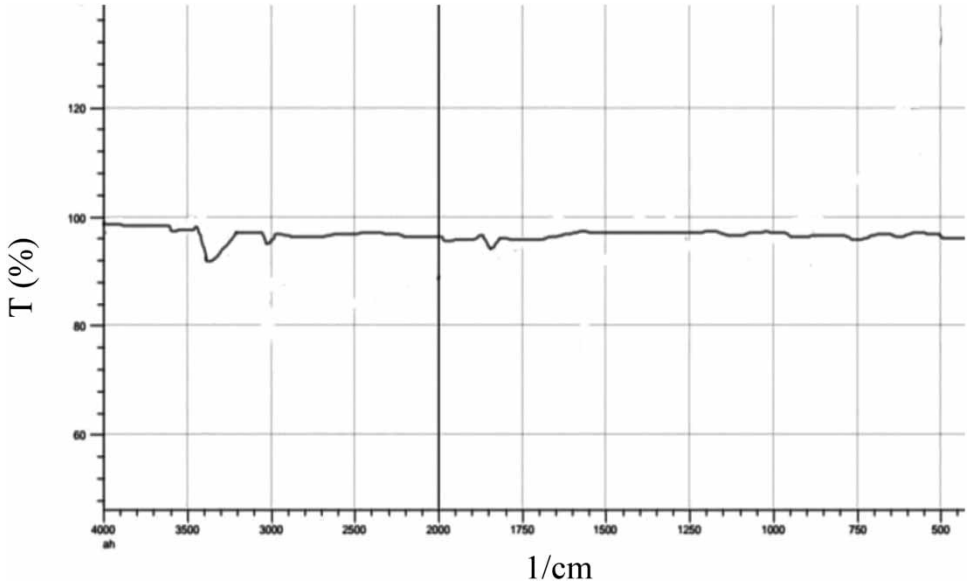

Figure 2 | The spectrum of FT-IR for the nano-activated carbon.

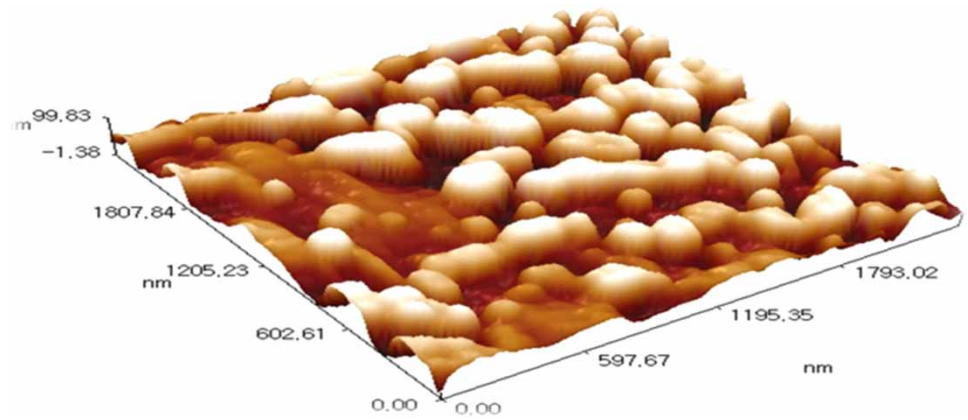

Figure 3 | AFM analysis of the surfaces of the developed activated carbon.

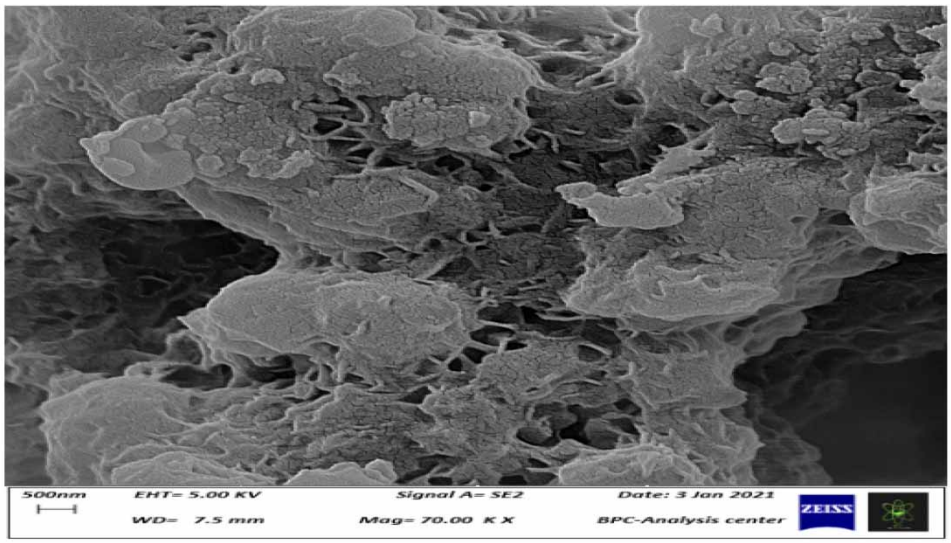

Figure 4 | SEM analysis of the surface of the activated carbon.

3.1.4. Energy-dispersive X-ray spectroscopy

Additionally, X-ray technology was used to characterize the new activated carbon. The results of this analysis show in Figure 4 that the activated carbon's chemical composition is made from carbon (78.57%) and oxygen (21.43%), which confirms the activity of the activated carbon as an adsorbent Figure 5.

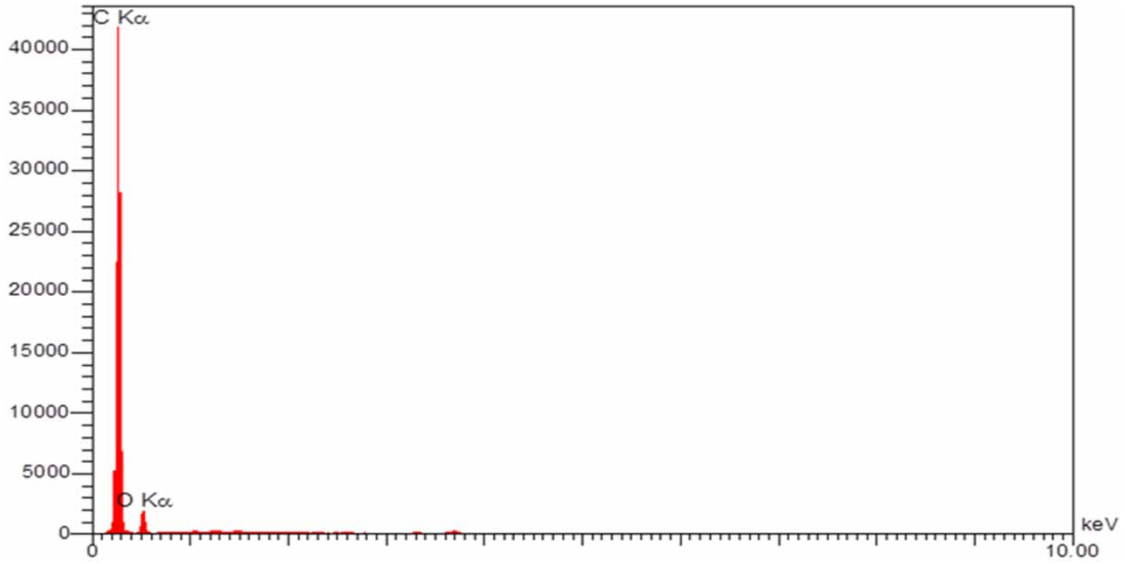

Figure 5 | Results of the X-ray analysis of the activated carbon.

The results of the measurement of sizes of pores and voids on the surfaces of the activated carbon that was prepared using the BJH (Barrett-Joyner–Halenda) method are shown in Table 1. It can be seen from these results that the average width of the pores is 1.21 nm, and the surface area (after carbonization) is about 1,071.7 m^2/mg. The presence of hyperbranched in the structure of the activated carbon gives it an important feature: the captured ions or atoms in these pores will not be able to escape these pores.

Table 1 | BET measurement before and after mixing the banana peels, nylon 66 and polyethene

Banana peels only (BET)	Width of pores before carbonization	BET after carbonization (polyethene + nylon 66)	Width of pores after carbonization
1,389.9 m^2/mg	1.21 nm	1,071.7 m^2/mg	1.21 n m

It should be mentioned that the purpose of mixing polyethene and nylon 66 with the peels of banana is decomposing of nylon and removal of hydrogen from activated carbon, and reconnection of the formed parts of the mixture with the free amine. These reactions occur in alkaline media and help to decompose the original materials and reform the produced parts.

3.2. Dye adsorption

Results of Table 2 and Figures 5–8 deliver essential information about the efficiency of the activated carbon. For example, it can be seen that adding polyethene and nylon 66 to the banana peels increases the voids ratio on the surface of the new activated carbon. Previous studies showed that adding polyethene alone to the mixture could decrease the pores on the surface of the peels of banana, while other studies stated that adding nylon 66 alone to the peels of banana increases the pores on the surface of the produced carbon (Awalgaonkar *et al.* 2020).

The present study showed that mixing polyethene and nylon 66 and adding them to the peels of banana significantly increased the pores on the surface of the activated carbon, which was proved by the adsorption of methylene dye, as shown in Table 2. Additionally, the iodine number during the adsorption of iodine dye was good.

Table 2 | Values of key parameters obtained from mixing nylon 66, polyethene and banana peels

Sample	The ratio of banana: KOH: nylon + poly	IN mg/gm	Methylene Blue 2 mg/gm	λ	Ash %	Density gm/cm^3	Cinders %	Humidity %
1	1 : 2 : 0.1	297.7	24	665	0.264	0.25	0.68	12.8
2	1 : 2 : 0.2	417.7	50.7	665	0.390	0.52	0.61	26.4
3	1 : 2 : 0.3	599.1	61.87	665	0.465	0.27	3.02	13.5
4	1 : 2 : 0.4	620.6	76.7	665	0.243	0.294	1.61	14.7

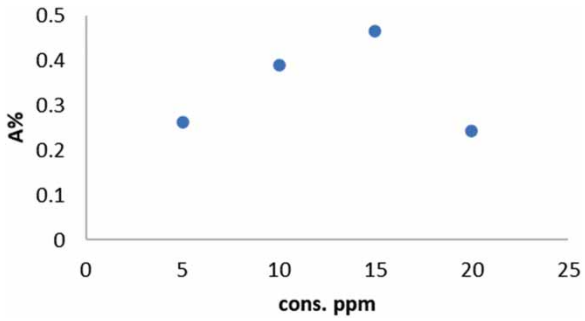

Figure 6 | Methylene Blue dye adsorption on the produced activated carbon.

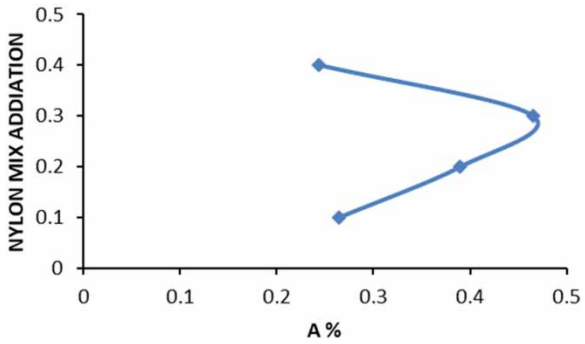

Figure 7 | Effect of nylon addition on the adsorption capacity of activated carbon.

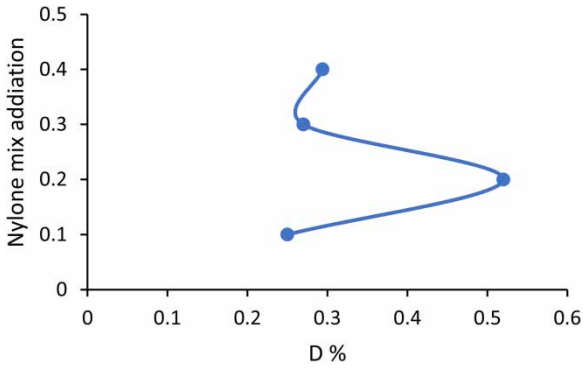

Figure 8 | Effect of nylon addition on the density of activated carbon.

The measurement of activated carbon density showed that the density was not stable (increase and decrease) due to the difficult separation of groups and their carrier media.

An increase in the moisture indicates the activity of the produced carbon.

The results of this study, in summary, proved the activity of the produced carbon, its high porosity, its high efficiency in the removal of pollutants, and also indicated the produced activated carbon is free of toxic elements, such as sulfate and nitrogen.

Also, the results showed that by using different concentrations of activated charcoal before using the nanomaterials, the removal of methylene and EDT increased with the increase in the adsorbent dose.

The spectrum method was also used to assess the adsorption by the new activated carbon; the results of this method showed a linear relationship between the adsorption and the concentrations of the dye, as shown in Figure 9. Also, the results of this study showed the adsorption time for the new activated carbon ranged between 40 and 50 minutes, as shown in Table 3. Increasing the contact time was not useful because of the depletion of the pores on the surface of the new activated carbon.

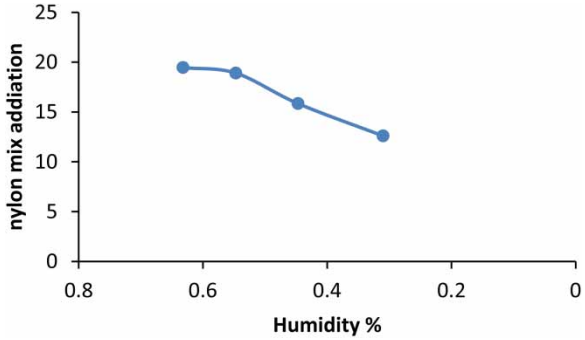

Figure 9 | Effect of nylon addition on the humidity.

Table 3 | Equilibrium time and efficiency of adsorption at 22 °C and dose of activated carbon of 0.04 g

Time	Abs.	Ads. %
0	0.318	–
10	0.172	81.00
20	0.151	86.44
30	0.148	91.00
40	0.144	93.22
50	0.144	93.22
60	0.145	90.88
70	0.147	89.78

The effects of the initial concentration of the pollutants and the dose of the adsorbent on the efficiency of the new activated carbon, are shown in Tables 4 and 5, respectively. The results showed 0.04 g of activated carbon and 20 ppm concentration of the dye achieved the best efficiency of the new carbon. The efficiency of the new activated carbon was calculated using the following equations:

$$Adsorption = \frac{C_o - C_e}{C_{o\times 100}} \tag{6}$$

$$Q_e = \frac{C_o - C_e}{M \times V} \tag{7}$$

Temperature effects on the equilibrium constant, as listed in Table 6, show increasing the temperature decreases the adsorption capacity. The thermodynamic functions were calculated, as listed in Table 7, to

Table 4 | Effect of initial concentration of EBT dye on the adsorption efficiency

C_o (ppm)	Abs. before adsorption	Abs. after adsorption	C_e (ppm)	Ads.%
20	0.318	0.144	2.123	93.22
40	0.411	0.135	28.234	87.57
60	0.589	0.205	34.465	81.12

Table 5 | Effect of activated carbon weight on the adsorption efficiency

Weight of AC (g)	Abs.	C_e (mg/L)	C_t (mg/g)	Adsorption%
0.01	0.168	5.000	23.998	80.49
0.02	0.155	3.913	25.893	84.88
0.04	0.144	2.123	26.339	93.22

Table 6 | Effect of temperature on the constant of the equilibrium state of the studied system

T (K)	A	1/T (K^{-1})	C_e (mg/L)	Ads %	lnK_{eq}
283.15	0.128	0.00353	27.144	94.87	2.788
293.15	0.136	0.00341	26.799	93.68	2.322
298.15	0.143	0.00335	26.062	89.97	2.006
203.15	0.189	0.00330	25.811	83.37	1.577
313.15	0.174	0.00319	23.318	77.99	1.487

Table 7 | Values of the thermodynamic functions of the dye adsorption on the surface of the prepared activated carbon

T (K)	ΔH° (kJ.$mole^{-1}$)	ΔG° (kJ.$mole^{-1}$)	ΔS° (kJ.$mole^{-1}$.K^{-1})
283.15	39.998-	−6.188	−119.400
293.15		−6.007	−115.950
298.15		−5.578	−115.445
303.15		−4.142	−118.278
313.15		−3.986	−114.999

define the nature of the adsorption system:

$$\Delta G = \Delta H - T\Delta \tag{8}$$

$$\text{Log } K = (-\Delta H / 2.303\, RT) + C \tag{9}$$

where K, R and C represent the highest adsorbed amount, gases constant, and integration constant, respectively.

The free energy value was calculated using the following equation:

$$\Delta G = -RT\, Ln(Qe/Ce) \tag{10}$$

where Ce and Qe represent the concentration at the equilibrium, and the adsorbed amount, respectively.

Figure 10 shows the best peak at which the dye is absorbed. Through the best wavelength (530 nm), the calibration curve (Figure 10) found that the adsorption process is subject to the pseudo-second-order equation according to the correlation coefficient R2 with a value of (0.997).

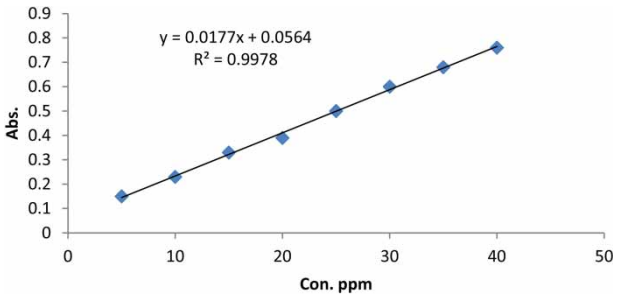

Figure 10 | Standard calibration curve of adsorption of EBT dye.

From the results obtained from the UV tests, it was found that the best peak at which the EBT dye was absorbed took placed at a wavelength of 530 nm, and according to the calibration curve (Figure 10), the adsorption process is subjected to a second-order false equation (according to the correlation coefficient R^2, which has a value of 0.9978).

The negative sign of ΔH indicates the adsorption process of the EBT dye on the new nano-carbon was an exothermic process; the adsorption physically occurs because it is less than 40 KJ/mole. Additionally, the change in the value of the free energy (ΔG) indicates the reaction happens automatically (spontaneously), and the negative value of $\Delta \cdot S$ indicates the reduction in the randomness of the process, as shown in Table 7.

Any adsorption media is subjected to depletion after a certain period of service; therefore, it is important to use an efficient monitoring tool to avoid the effects of the depletion on the performance of the adsorption unit. In this study, microwave sensing systems are recommended for the monitoring of depletion in the nanoparticle filters. The microwave sensing system was recommended because of its past successful applications; for example, it was used in the monitoring of health structures (Gkantou *et al.* 2019; Teng *et al.* 2019; Kot *et al.* 2021a), non-destructive sensing (Kot *et al.* 2021b; Omer *et al.* 2021), communications (Ryecroft *et al.* 2019a; Ryecroft *et al.* 2021), water pollution monitoring (Ryecroft *et al.* 2019b).

4. CONCLUSION

The present study focused on the development of nano-activated carbon from banana peels that mixed some additives (nylon 6.6 and polyethene). Additionally, this study aims at the application of the developed nano-activated carbon to remove dyes from water. The findings of this study indicated the nano-activated carbon has spherical particles with a pore size of 1.21 nm and a surface area of 1,071.7 m^2/gm. Additionally, it was noticed that the prepared carbon does not contain any active groups, which means it is an inert material. Additionally, the results showed the nano-activated carbon has a good ability to remove dyes from water; the best equilibrium time dose of carbon and concentration of dyes was 40–50 minutes, 0.04 g and 20 ppm, respectively. It was also noticed that the adsorption efficiency decreases with the increase of the temperature; the adsorption was exothermic and with low randomness.

For future studies, a detailed investigation of the effects of solution pH on the adsorption of dyes by nano-carbon should be performed.

DATA AVAILABILITY STATEMENT

Data cannot be made publicly available; readers should contact the corresponding author for details.

REFERENCES

Abatan, O. G., Oni, B. A., Agboola, O., Efevbokhan, V. & Abiodun, O. O. 2019 Production of activated carbon from African star apple seed husks, oil seed and whole seed for wastewater treatment. *Journal of Cleaner Production* **232**, 441–450.

Abdulhadi, B. A., Kot, P., Hashim, K. S., Shaw, A. & Khaddar, R. A. 2019 Influence of current density and electrodes spacing on reactive red 120 dye removal from dyed water using electrocoagulation/electroflotation (EC/EF) process. In: *First International Conference on Civil and Environmental Engineering Technologies (ICCEET)*. University of Kufa, Iraq, pp. 12–22.

Abdulhadi, B., Kot, P., Hashim, K., Shaw, A., Muradov, M. & Al-Khaddar, R. 2021 Continuous-flow electrocoagulation (EC) process for iron removal from water: experimental, statistical and economic study. *Science of the Total Environment* **760**(2), 1–16.

Abdulla, G., Kareem, M. M., Hashim, K. S., Muradov, M., Kot, P., Mubarak, H. A., Abdellatif, M. & Abdulhadi, B. 2020 Removal of iron from wastewater using a hybrid filter. In: *IOP Conference Series: Materials Science and Engineering*. IOP Publishing, p. 012035.

Abdulraheem, F. S., Al-Khafaji, Z. S., Hashim, K. S., Muradov, M., Kot, P. & Shubbar, A. A. 2020 Natural filtration unit for removal of heavy metals from water. In: *IOP Conference Series: Materials Science and Engineering*. IOP Publishing, p. 012034.

Abdullah, A. M., Alwan, L. H. & Abdulqader, A. M. 2020 Thermodynamic and kinetic studies of Eriochrome black adsorption on activated charcoal prepared from lemon leaves. *Materials Research Express* **6**(12), 1250h8.

Alenazi, M., Hashim, K. S., Hassan, A. A., Muradov, M., Kot, P. & Abdulhadi, B. 2020 Turbidity removal using natural coagulants derived from the seeds of *strychnos potatorum*: statistical and experimental approach. In: *IOP Conference Series: Materials Science and Engineering*. IOP Publishing, p. 012064.

Alenezi, A. K., Hasan, H. A., Hashim, K. S., Amoako-Attah, J., Gkantou, M., Muradov, M., Kot, P. & Abdulhadi, B. 2020 Zeolite-assisted electrocoagulation for remediation of phosphate from calcium-phosphate solution. In: *IOP Conference Series: Materials Science and Engineering*. IOP Publishing, p. 012031.

Al-Hashimi, O., Hashim, K., Loffill, E., Marolt Čebašek, T., Nakouti, I., Faisal, A. A. & Al-Ansari, N. 2021 A comprehensive review for groundwater contamination and remediation: occurrence, migration and adsorption modelling. *Molecules* **26**(19), 5913.

Alhendal, M., Nasir, M. J., Hashim, K. S., Amoako-Attah, J., Al-Faluji, D., Muradov, M., Kot, P. & Abdulhadi, B. 2020 Cost-effective hybrid filter for remediation of water from fluoride. In: *IOP Conference Series: Materials Science and Engineering*. IOP Publishing, p. 012038.

Al-Jumeily, D., Hashim, K., Alkaddar, R., Al-Tufaily, M. & Lunn, J. 2019 Sustainable and Environmental Friendly Ancient Reed Houses (Inspired by the Past to Motivate the Future). In; *11th International Conference on Developments in eSystems Engineering (DeSE)*. Cambridge, UK, pp. 214–219.

Al-Marri, S., AlQuzweeni, S. S., Hashim, K. S., AlKhaddar, R., Kot, P., AlKizwini, R. S., Zubaidi, S. L. & Al-Khafaji, Z. S. 2020 Ultrasonic-Electrocoagulation method for nitrate removal from water. In: *IOP Conference Series: Materials Science and Engineering*. IOP Publishing, p. 012073.

Alnaimi, H., Idan, I. J., Al-Janabi, A., Hashim, K., Gkantou, M., Zubaidi, S. L., Kot, P. & Muradov, M. 2020 Ultrasonic-electrochemical treatment for effluents of concrete plants. In: *IOP Conference Series Materials Science and Engineering*. University of Kufa, Najaf, Iraq, pp. 1–9.

Al-Saati, N. H., Hussein, T. K., Abbas, M. H., Hashim, K., Al-Saati, Z. N., Kot, P., Sadique, M., Aljefery, M. H. & Carnacina, I. 2019 Statistical modelling of turbidity removal applied to non-toxic natural coagulants in water treatment: a case study. *Desalination and Water Treatment* **150**, 406–412.

Al-Saati, N. H., Omran, I. I., Salman, A. A., Al-Saati, Z. & Hashim, K. S. 2021 Statistical modeling of monthly streamflow using time series and artificial neural network models: Hindiya Barrage as a case study. *Water Practice and Technology* **16**(2), 681–691.

Al-Sareji, O. J., Grmasha, R. A., Salman, J. M., Idowu, I. & Hashim, K. S. 2021 Street dust contamination by heavy metals in Babylon governorate, Iraq. *Journal of Engineering Science and Technology* **16**(1), 3528–3546.

Alyafei, A., AlKizwini, R. S., Hashim, K. S., Yeboah, D., Gkantou, M., Al Khaddar, R., Al-Faluji, D. & Zubaidi, S. L. 2020 Treatment of effluents of construction industry using a combined filtration-electrocoagulation method. In: *IOP Conference Series: Materials Science and Engineering*. IOP Publishing, p. 012032.

Aqeel, K., Mubarak, H. A., Amoako-Attah, J., Abdul-Rahaim, L. A., Al Khaddar, R., Abdellatif, M., Al-Janabi, A. & Hashim, K. S. 2020 Electrochemical removal of brilliant green dye from wastewater. In: *IOP Conference Series: Materials Science and Engineering*. IOP Publishing, p. 012036.

Awalgaonkar, G., Beaudry, R. & Almenar, E. 2020 Ethylene-removing packaging: basis for development and latest advances. *Comprehensive Reviews in Food Science and Food Safety* **19**(6), 3980–4007.

Efeovbokhan, V. E., Alagbe, E. E., Odika, B., Babalola, R., Oladimeji, T. E., Abatan, O. G. & Yusuf, E. O. 2019 Preparation and characterization of activated carbon from plantain peel and coconut shell using biological activators. In: *Journal of Physics: Conference Series*. IOP Publishing, p. 032035.

Ekpete, O., Marcus, A. & Osi, V. 2017 Preparation and characterization of activated carbon obtained from plantain (*Musa paradisiaca*) fruit stem. *Journal of Chemistry* **2017**, 1–6.

El-Sayed, G. O., Yehia, M. M. & Asaad, A. A. 2014 Assessment of activated carbon prepared from corncob by chemical activation with phosphoric acid. *Water Resources and Industry* **7**, 66–75.

Emamjomeh, M. M., Kakavand, S., Jamali, H. A., Alizadeh, S. M., Safdari, M., Mousavi, S. E. S., Hashim, K. S. & Mousazade, M. 2020a The treatment of printing and packaging wastewater by electrocoagulation–flotation: the simultaneous efficacy of critical parameters and economics. *Desalination and Water Treatment* **205**, 161–174.

Emamjomeh, M. M., Mousazadeh, M., Mokhtari, N., Jamali, H. A., Makkiabadi, M., Naghdali, Z., Hashim, K. S. & Ghanbari, R. 2020b Simultaneous removal of phenol and linear alkylbenzene sulfonate from automotive service station wastewater: optimization of coupled electrochemical and physical processes. *Separation Science and Technology* **55**(17), 3184–3194.

Farhan, S. L., Hashim, I. A. J. & Naji, A. A. 2019 The Sustainable House: Comparative Analysis of Houses in Al Kut Neighborhoods-Iraq. In: *2019 12th International Conference on Developments in ESystems Engineering (DeSE)*. IEEE, pp. 1031–1036.

Farhan, S. L., Antón, D., Akef, V. S., Zubaidi, S. L. & Hashim, K. S. 2021 Factors influencing the transformation of Iraqi holy cities: the case of Al-Najaf. *Scientific Review Engineering and Environmental Sciences* **30**(2), 365–375.

Foo, K. & Hameed, B. 2009 Utilization of biodiesel waste as a renewable resource for activated carbon: application to environmental problems. *Renewable and Sustainable Energy Reviews* **13**(9), 2495–2504.

Gkantou, M., Muradov, M., Kamaris, G. S., Hashim, K., Atherton, W. & Kot, P. 2019 Novel electromagnetic sensors embedded in reinforced concrete beams for crack detection. *Sensors* **19**(23), 5175–5189.

Grmasha, R. A., Al-sareji, O. J., Salman, J. M., Hashim, K. S. & Jasim, I. A. 2020 Polycyclic aromatic hydrocarbons (PAHs) in urban street dust within three land-uses of Babylon governorate, Iraq: distribution, sources, and health risk assessment. *Journal of King Saud University – Engineering Sciences* **33**, 1–18.

Hashim, K. S., Al-Saati, N. H., Hussein, A. H. & Al-Saati, Z. N. 2018 An investigation into the level of heavy metals leaching from canal-dreged sediment: a case study metals leaching from dreged sediment. In: *First International Conference on Materials Engineering & Science*. Istanbul Aydın University (IAU), Turkey, pp. 12–22.

Hashim, K. S., Al-Saati, N. H., Alquzweeni, S. S., Zubaidi, S. L., Kot, P., Kraidi, L., Hussein, A. H., Alkhaddar, R., Shaw, A. & Alwash, R. 2019a Decolourization of dye solutions by electrocoagulation: an investigation of the effect of operational parameters. In: *First International Conference on Civil and Environmental Engineering Technologies (ICCEET)*. University of Kufa, Iraq, pp. 25–32.

Hashim, K. S., Hussein, A. H., Zubaidi, S. L., Kot, P., Kraidi, L., Alkhaddar, R., Shaw, A. & Alwash, R. 2019b Effect of initial pH value on the removal of reactive black dye from water by electrocoagulation (EC) method. In: *2nd International Scientific Conference*. Al-Qadisiyah University, Iraq, pp. 12–22.

Hashim, K., Kot, P., Zubaid, S., Alwash, R., Al Khaddar, R., Shaw, A., Al-Jumeily, D. & Aljefery, M. 2020a Energy efficient electrocoagulation using baffle-plates electrodes for efficient escherichia coli removal from wastewater. *Journal of Water Process Engineering* **33**(20), 101079–86.

Hashim, K. S., Ali, S. S. M., AlRifaie, J. K., Kot, P., Shaw, A., Al Khaddar, R., Idowu, I. & Gkantou, M. 2020b Escherichia coli inactivation using a hybrid ultrasonic–electrocoagulation reactor. *Chemosphere* **247**, 125868–75.

Hashim, K. S., AlKhaddar, R., Shaw, A., Kot, P., Al-Jumeily, D., Alwash, R. & Aljefery, M. H. 2020c Electrocoagulation as an eco-friendly river water treatment method. In: *Advances in Water Resources Engineering and Management* (Alkhaddar, R., (ed.)). Springer, Berlin.

Hashim, K. S., Ewadh, H. M., Muhsin, A. A., Zubaidi, S. L., Kot, P., Muradov, M., Aljefery, M. & Al-Khaddar, R. 2021a Phosphate removal from water using bottom ash: adsorption performance, coexisting anions and modelling studies. *Water Science and Technology* **83**(1), 77–89.

Hashim, K. S., Shaw, A., AlKhaddar, R., Kot, P. & Al-Shamma'a, A. 2021b Water purification from metal ions in the presence of organic matter using electromagnetic radiation-assisted treatment. *Journal of Cleaner Production* **280**(2), 1–17.

Kot, P., Hashim, K. S., Muradov, M. & Al-Khaddar, R. 2021a How can sensors be used for sustainability improvement?. In: *Methods in Sustainability Science*, 1st edn (Hayton, J., ed.). Elsevier, United Kingdom, p. 426.

Kot, P., Muradov, M., Gkantou, M., Kamaris, G. S., Hashim, K. & Yeboah, D. 2021b Recent advancements in non-destructive testing techniques for structural health monitoring. *Applied Sciences* **11**(6), 1–28.

Lim, W. C., Srinivasakannan, C. & Balasubramanian, N. 2010 Activation of palm shells by phosphoric acid impregnation for high yielding activated carbon. *Journal of Analytical and Applied Pyrolysis* **88**(2), 181–186.

Mohammed, A.-H., Hussein, A. H., Yeboah, D., Al Khaddar, R., Abdulhadi, B., Shubbar, A. A. & Hashim, K. S. 2020 Electrochemical removal of nitrate from wastewater. In: *IOP Conference Series: Materials Science and Engineering*. IOP Publishing, p. 012037.

Omer, G., Kot, P., Atherton, W., Muradov, M., Gkantou, M., Shaw, A., Riley, M., Hashim, K. & Al-Shamma'a, A. 2021 A non-destructive electromagnetic sensing technique to determine chloride level in maritime concrete. *Karbala International Journal of Modern Science* **7**(1), 61–71.

Omran, I. I., Al-Saati, N. H., Hashim, K. S., Al-Saati, Z. N., Patryk, K., Khaddar, R. A., Al-Jumeily, D., Shaw, A., Ruddock, F. & Aljefery, M. 2019 Assessment of heavy metal pollution in the Great Al-Mussaib irrigation channel. *Desalination and Water Treatment* **168**, 165–174.

Omran, I. I., Al-Saati, N. H., Al-Saati, H. H., Hashim, K. S. & Al-Saati, Z. N. 2021 Sustainability assessment of wastewater treatment techniques in urban areas of Iraq using multi-criteria decision analysis (MCDA). *Water Practice and Technology* **16**(2), 648–660.

Ozdemir, I., Şahin, M., Orhan, R. & Erdem, M. 2014 Preparation and characterization of activated carbon from grape stalk by zinc chloride activation. *Fuel Processing Technology* **125**, 200–206.

Rahimian, R. & Zarinabadi, S. 2020 A review of studies on the removal of methylene blue dye from industrial wastewater using activated carbon adsorbents made from almond bark. *Progress in Chemical and Biochemical Research* **3**(3), 251–268.

Ryecroft, S., Shaw, A., Fergus, P., Kot, P., Hashim, K., Moody, A. & Conway, L. 2019a A first implementation of underwater communications in raw water using the 433 MHz frequency combined with a bowtie antenna. *Sensors* **19**(8), 1813–1823.

Ryecroft, S. P., Shaw, A., Fergus, P., Kot, P., Hashim, K. & Conway, L. 2019b A Novel Gesomin Detection Method Based on Microwave Spectroscopy. In: *12th International Conference on Developments in ESystems Engineering (DeSE)*, Kazan, Russia, pp. 429–433.

Ryecroft, S., Shaw, A., Fergus, P., Kot, P., Hashim, K., Tang, A., Moody, A. & Conway, L. 2021 An implementation of a multi-hop underwater wireless sensor network using bowtie antenna. *Karbala International Journal of Modern Science* **7**(2), 113–129.

Salah, Z., Abdulkareem, I. H., Hashim, K. S., Al-Bugharbee, H., Ridha, H. M., Gharghan, S. K., Al-Qaim, F. F., Muradov, M., Kot, P. & Alkhaddar, R. 2020a Hybridised artificial neural network model with slime mould algorithm: a novel methodology for prediction urban stochastic water demand. *Water* **12**(10), 1–18.

Salah, Z., Hashim, K., Ethaib, S., Al-Bdairi, N. S. S., Al-Bugharbee, H. & Gharghan, S. K. 2020b A novel methodology to predict monthly municipal water demand based on weather variables scenario. *Journal of King Saud University-Engineering Sciences* **32**(7), 1–18.

Salah, Z., Ortega-Martorell, S., Kot, P., Alkhaddar, R. M., Abdellatif, M., Gharghan, S. K., Ahmed, M. S. & Hashim, K. 2020c A method for predicting long-term municipal water demands under climate change. *Water Resources Management* **34**(3), 1265–1279.

Stoeckli, H. F. 1990 Microporous carbons and their characterization: the present state of the art. *Carbon* **28**(1), 1–6.

Taha, N., Abdelhafez, S. & El-Maghraby, A. 2016 Chemical and physical preparation of activated carbon using raw bagasse pith for cationic dye adsorption. *Global Nest Journal* **18**(2), 402–415.

Teng, K. H., Kot, P., Muradov, M., Shaw, A., Hashim, K., Gkantou, M. & Al-Shamma'a, A. 2019 Embedded smart antenna for non-destructive testing and evaluation (NDT&E) of moisture content and deterioration in concrete. *Sensors* **19**(3), 547–559.

Yamaguchi, A., Watanabe, T., Saito, K., Kuwano, S., Murakami, Y., Mimura, N. & Sato, O. 2019 Direct conversion of lignocellulosic biomass into aromatic monomers over supported metal catalysts in supercritical water. *Molecular Catalysis* **477**, 110557.

Zanki, A. K., Mohammad, F. H., Hashim, K. S., Muradov, M., Kot, P., Kareem, M. M. & Abdulhadi, B. 2020 Removal of organic matter from water using ultrasonic-assisted electrocoagulation method. In: *IOP Conference Series: Materials Science and Engineering*. IOP Publishing, p. 012033.

Zhong, Z.-Y., Yang, Q., Li, X.-M., Luo, K., Liu, Y. & Zeng, G.-M. 2012 Preparation of peanut hull-based activated carbon by microwave-induced phosphoric acid activation and its application in Remazol Brilliant Blue R adsorption. *Industrial Crops and Products* **37**(1), 178–185.

Zhongfu, L. 1991 Theoretic analyze and experiments of solar-powered refrigeration with solid adsorption pal RS. *Journal of Refrigeration* **4**, 1–14.

Zubaidi, S. L., Al-Bugharbee, H., Muhsen, Y. R., Hashim, K., Alkhaddar, R. M., Al-Jumeily, D. & Aljaaf, A. J. 2019 The Prediction of Municipal Water Demand in Iraq: A Case Study of Baghdad Governorate. In: *12th International Conference on Developments in ESystems Engineering (DeSE)*, Kazan, Russia, pp. 274–277.

Zubaidi, S., Al-Bugharbee, H., Muhsin, Y. R., Hashim, K. & Alkhaddar, R. 2020a Forecasting of monthly stochastic signal of urban water demand: Baghdad as a case study. In: *IOP Conference Series: Materials Science and Engineering*. IOP Publishing, p. 012018.

Zubaidi, S., Ortega-Martorell, S., Al-Bugharbee, H., Olier, I., Hashim, K. S., Gharghan, S. K., Kot, P. & Al-Khaddar, R. 2020b Urban water demand prediction for a city that suffers from climate change and population growth: Gauteng province case study. *Water* **12**(7), 1–18.

Zubaidi Salah, L., Al-Bugharbee, H., Ortega Martorell, S., Gharghan, S., Olier, I., Hashim, K., Al-Bdairi, N. & Kot, P. 2020 A novel methodology for prediction urban water demand by wavelet denoising and adaptive neuro-fuzzy inference system approach. *Water* **12**(6), 1–17.

First received 11 September 2021; accepted in revised form 17 October 2021. Available online 28 October 2021